Fabrication of subwavelength, binary, antireflection surface-relief structures in the near infrared

J. R. Wendt,[a] G. A. Vawter, R. E. Smith, and M. E. Warren
Sandia National Laboratories, Albuquerque, New Mexico 87185-0603

(Received 28 May 1996; accepted 12 August 1996)

Subwavelength, binary surface-relief structures are artificial materials with an effective index of refraction that can be tailored by varying the duty cycle of the binary pattern. These structures have the significant advantage of requiring only a single lithography and etch step for fabrication. We demonstrate a specifically designed antireflection structure in a material system (GaAs) and at a wavelength (975 nm) directly integrable with GaAs-based vertical cavity surface-emitting lasers and which exhibits strong polarization-dependent properties. Fabrication is performed using electron beam lithography and reactive-ion-beam etching. The observed reflectivity is 2% for TE polarization and 23% for TM polarization, a difference in reflectivity of over a factor of 10 for the two polarizations. © *1996 American Vacuum Society.*

I. INTRODUCTION

Subwavelength, binary surface-relief structures act as artificial materials whose effective index of refraction depends on the fill factor of the binary pattern. Subwavelength structures have the significant advantage over conventional multilevel diffractive optics of requiring only a single lithography and etch step for fabrication. The simplest subwavelength structure to analyze is that of a one-dimensional (1-D), rectangular-profile grating with periodicity less than the wavelength of light in the material, as shown in Fig. 1(a). This is a zero-order grating which transmits (and reflects) only the zeroth diffracted order, without change in the direction of propagation, analogous to light transmission through (and reflection from) a homogenous material. We use the general term "structure" instead of the more common term "grating" to refer to the subwavelength surface-relief pattern of this work to emphasize that it does not act as a conventional diffraction grating, but, rather, as an artificial material with a variety of interesting and useful properties. With the proper choice of fill factor and thickness, and for a given polarization, the 1-D structure exhibits antireflection (AR) behavior directly analogous to the quarterwave AR coating, as shown in Fig. 1(b). The antireflection property has broad application in micro-optics and in semiconductor-based optoelectronic systems, particularly at wavelengths where appropriate conventional AR coatings may not exist.

The polarization dependence of the antireflection property arises from the lack of rotational symmetry in the 1-D AR structure and has direct application to polarization control in vertical-cavity surface-emitting lasers (VCSELs), which consist of an optical gain region sandwiched between two mirrors, typically distributed Bragg reflectors. VCSELs have many desirable properties including the ability to have circular output beams and for fabrication in two-dimensional arrays. One potential problem for VCSELs with some type of symmetry in the shape of the output aperture (e.g., circular or square apertures) is that the axis of polarization of the output beam is random, although typically aligned to either of two orthogonal crystal directions.[1] Another concern is that the axis of polarization is observed to switch between the two orthogonal orientations as a function of injection current.[1] The ability to control the axis of polarization would be vital for any optical system containing polarization-sensitive elements or using the state of polarization to convey coded information. The integration of a subwavelength structure which exhibits polarization-dependent reflectivity with a conventional VCSEL should lead to a device which lases with the axis of polarization aligned to the high-reflectivity axis of the 1-D subwavelength structure.

Another property of this 1-D AR structure is that of form birefringence,[2] which is the presence of polarization-dependent indices of refraction arising from the anisotropy of the subwavelength geometry of the 1-D AR structure (as opposed to simple birefringence arising from anisotropy in the electronic structure on a molecular scale in a crystalline material). The magnitude of the difference between the indices of refraction for the two orthogonal polarizations increases as the difference between the indices of the incident and substrate materials of Fig. 1 increases. The presence of form birefringence in these 1-D surfaces may be exploited to create waveplates which can be used to alter states or axes of polarization.

Various theoretical and experimental treatments of subwavelength AR surfaces have appeared in the literature.[3–9] Early experimental work by Flanders[3] demonstrated birefringence in 1-D, rectangular-profile gratings in polymethylmethacrylate (PMMA) and silicon nitride, and its dependence on fill factor and thickness, at a wavelength of 633 nm. Enger and Case[4] demonstrated antireflection behavior in 1-D, triangular-profile gratings in quartz at 633 nm. Gaylord, Baird, and Moharam[5] provided a rigorous theoretical treatment of 1-D, rectangular-profile gratings valid even for the regime where the grating period is of the same order as the incident wavelength. Ono *et al.*[6] reported a model for the observed AR behavior of 1-D, sinusoidal- and triangular-profile gratings in photoresist at 633 nm. Cescato, Gluch, and

[a]Electronic mail: jrwendt@sandia.gov

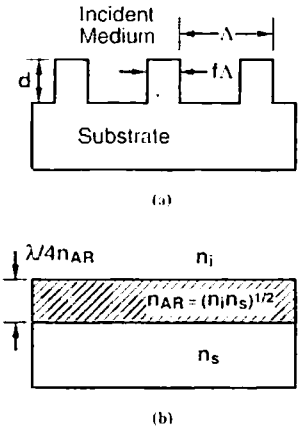

FIG. 1. (a) Schematic representation of a one-dimensional, rectangular-profile grating with pitch Λ, depth d, fill factor f, and rib width $f\Lambda$. (b) ...gn for a standard quarterwave antireflection layer.

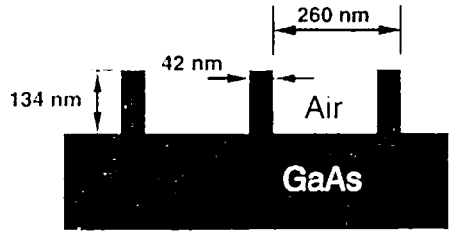

FIG. 2. Design for the antireflection surface-relief structure. The pitch is 260 nm, the rib width is 42 nm, and the etch depth is 134 nm.

Streibl[7] studied birefringence in 1-D, sinusoidal-profile gratings in photoresist at 633 nm. Raguin and Morris[8] made an extensive theoretical investigation of 1-D, triangular-profile gratings and two-dimensional, pyramidal-profile gratings in GaAs at 10.6 μm. Finally, Deng and Chou[9] have reported properties of 1-D, nominally trapezoidal-profile gratings as a function of grating period in amorphous silicon on silica at 633 nm.

In this work, we demonstrate a specifically designed antireflection structure in a material system (GaAs) and at a wavelength (975 nm) directly integrable with GaAs-based VCSELs and which exhibits strong polarization-dependent properties. To our knowledge, this AR surface is fabricated in the highest refractive index material ($n_{GaAs}=3.5$) and has the smallest feature sizes (~ 50 nm) yet reported. Fabrication is performed using electron beam lithography and reactive-...on-beam etching. The main challenge in fabrication is ...chieving the specific sub-tenth micron linewidths and controlling the etch profiles and depths. We observe excellent agreement between our theoretical calculations and our experimental measurements.

II. DESIGN

Our AR surface is designed for fabrication in GaAs and for operation at 975 nm with normal incidence. The period of the AR surface, $\Lambda = 260$ nm, is chosen to be just slightly less than the wavelength of 975 nm light in GaAs so that only the zero-diffracted order will propagate in the material. The goal of the design is to create an AR surface analogous to a conventional quarterwave AR thin film. For an air/GaAs interface, the AR layer would have a refractive index, $n_{AR} = (n_{GaAs})^{1/2} = 1.87$, and a thickness, $t = \lambda/(4n_{AR}) = 130$ nm. The AR surface designed for this work, then, is an artificial material whose effective index of refraction is 1.87. Since we are designing a periodic, rectangular-profile structure, the only parameter to be determined is the fill factor, f, of the binary pattern, or, alternatively, the width of the ribs which comprise the AR surface, indicated by $f\Lambda$ in Fig. 1. Because the period is only slightly smaller than the wavelength of light in the material, a more accurate calculation than the simple effective medium theory[2] (EMT) should be used. We began by using a set of transcendental equations for the effective index of the fundamental eigenmode propagating parallel to the layers of an infinite periodic medium.[10] The result of these equations was then used as the starting point for direct optimization using a full vector Fourier method. Further details of the design methodology are provided elsewhere.[11,12] The results of the design calculation are shown schematically in Fig. 2. The design rib width of 42 nm corresponds to a fill factor of 0.16 compared to a fill factor of 0.22 which is obtained from the simple EMT approximation. This design has a theoretical transmission of 100% for TE-polarized light (electric field parallel to the grating ribs), and 74% for TM-polarized light (electric field perpendicular to grating ribs). For comparison, the transmission through an air/GaAs interface (for normal incidence at 975 nm wavelength) is $\sim 71\%$ and is polarization independent.

III. FABRICATION

The nanometer-scale dimensional requirements of the above design were achieved using electron beam lithography and reactive-ion-beam etching (RIBE) with a Ni/SiO_2 mask. The fabrication procedure used is a modified version of that which we reported previously for the fabrication of a subwavelength, blazed transmission grating.[13] Several of the process parameters had to be optimized to achieve the ~ 50 nm feature sizes. The front side of the bulk GaAs wafer was coated first with 100 nm of plasma-deposited SiO_2 and then spin-coated with 100 nm of PMMA electron beam resist. Following electron beam patterning of the PMMA, 5 nm of titanium (for adhesion) and 35 nm of nickel were evaporated onto the sample and the unwanted metal lifted-off. The Ti/Ni pattern was transferred first into the SiO_2 layer by reactive-ion etching (RIE) and then into the GaAs surface by RIBE. The fabrication steps are described in more detail below along with comments on the changes compared to the procedures of Ref. 13.

The electron beam lithography was performed on a JEOL JBX-5FE field emission system operating at 50 kV. A beam current of 500 pA, with a corresponding beam diameter of 6 nm, was used. The addressed pixel spacing was 5 nm in an

80 μm field. The PMMA thickness was reduced to 100 nm for increased resolution and the Ti/Ni thickness was correspondingly reduced to a total of 40 nm to maintain reliable liftoff. The reduction in mask thickness was not an issue because of the shallow etch depth (134 nm). The use of Ti instead of Cr arose from the observation of slightly better liftoff yield for Ti compared to Cr, but the difference was small. As with the blazed grating,[13] the challenge of this work is to achieve the design dimensions etched in GaAs which requires compensation for the proximity effect during exposure, linewidth increase during post-development oxygen descum, resist deformation during metal evaporation, and any lateral dimension changes while transferring the Ti/Ni pattern to the SiO_2 and GaAs. Because the pattern is periodic, all of the above effects operate uniformly across the pattern. Compensation for these effects can thereby be accomplished with an appropriately biased pattern written at a single, optimized dose. The desired 42-nm-wide rib pattern was biased down to 15 nm for exposure.

The overall AR pattern was written as a square, 960 μm on a side, to provide a large area for measurement. One may note that this structure is relatively insensitive to field stitch errors which simply perturb the local fill factor over a one-period distance at the stitch boundary. For this structure, the period is 0.26 μm and the field size is 80 μm, so the affected area is only 0.3% of the total area and typical field stitch errors are less than 10% of the period. Because of the spatial averaging process which determines the effective index, subwavelength structures, in general, are relatively insensitive to all random fabrication errors whose magnitudes are small compared to the subwavelength geometry and whose means are near zero averaged over small areas. The best dose range for the AR pattern was found to be 1000–1050 $\mu C/cm^2$. Development was performed for 50 sec in a 1:3 solution of methyl isobutyl ketone (MIBK) and isopropyl alcohol (IPA). After the Ti/Ni lift-off, the SiO_2 layer was etched using CHF_3/O_2 RIE. The GaAs was etched in a custom-built RIBE system with an electron cyclotron resonance (ECR) ion source. The etch gas was chlorine at a pressure of 2.5×10^{-4} Torr. The typical acceleration voltage and beam current density were 300 eV and 0.62 mA/cm^2, respectively. Etches were performed on a timed basis according to system calibration. A scanning electron micrograph of the cross section of three ribs of a fabricated AR surface is shown in Fig. 3. Typical measured rib widths are 55 ± 5 nm and etch depths are 140 ± 5 nm. Note the precise rectangular profiles achieved at this nanometer scale.

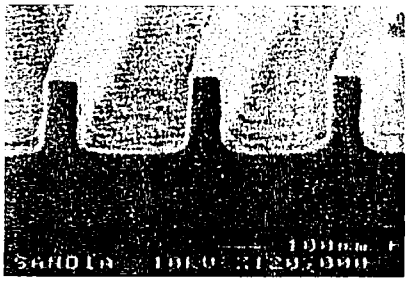

FIG. 3. Scanning electron micrograph of the cross section of a portion of the antireflection surface fabricated in GaAs.

IV. EXPERIMENTAL RESULTS

Characterization of the behavior of the AR surface was performed using the experimental setup diagrammed in Fig. 4. The front side of the wafer was coated with an opaque chrome layer everywhere except for the AR surface, forming a 960 μm square aperture. To further ensure that transmission through only the AR surface was measured, the incident laser light was also passed through a 960 μm square aperture prior to incidence on the back side of the wafer. Transmission measurements were made for both TE and TM polarization, at normal incidence, over a wavelength range of 960–990 nm. The measurement used a Ti–sapphire laser light source, a beam chopper, and lock-in detection. A small beam splitter was placed in close proximity to the sample to split off a reference beam for normalization of any power level fluctuations.

In order to determine the true performance of the AR surface, we need to separate the effects of the back side surface reflectivity and the optical absorption in the substrate. This can be accomplished by exploiting the information contained in the magnitude of the Fabry–Perot oscillations observed in the raw data. An asymmetric Fabry–Perot cavity is formed between the front and back air interfaces of the GaAs substrate. By assuming that the back side reflection and optical absorption are polarization independent, one may solve for the front side reflection for both TE and TM polarizations. Details of this calculation are reported elsewhere.[11] The measured transmission data for both TE and TM polarizations is shown in Fig. 5 along with theoretical values for a typical AR surface with rib width of 50 nm and etch depth of 135 nm. The agreement between experiment and theory is seen to be excellent, with measured values for transmission of 98% and 77% for TE and TM polarizations, respectively. Note that the design of the AR surface is relatively forgiving in that the significant percentage error ($\sim 30\%$) in the etched rib width compared to the design value results in only a 2%

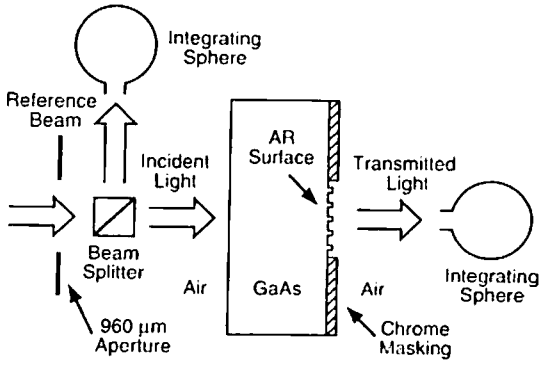

FIG. 4. Diagram of the experimental setup used for measuring the transmission through the antireflection surface.

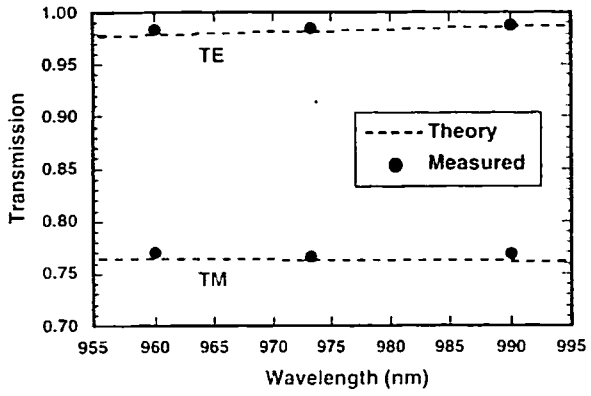

FIG. 5. Measured transmission through the antireflection surface for TE and TM polarizations along with theoretical values for a structure with rib width of 50 nm and etch depth of 135 nm.

reduction in transmission from the theoretical maximum. In terms of reflectivity, the value observed for TE-polarized light is 2% versus 23% for TM-polarized light. This greater than a factor of 10 polarization-dependent difference in reflectivity confirms the applicability of these AR surfaces to polarization control in VCSELs.

V. SUMMARY

We have demonstrated the design, fabrication, and characterization of a specific antireflection structure in a material system (GaAs) and at a wavelength (975 nm) directly integrable with GaAs-based vertical cavity surface-emitting lasers. The design technique utilized an effective index approximation valid for the range where the grating pitch is only slightly less than the wavelength in the material, in conjunction with a full vector Fourier method. Fabrication was performed using electron beam lithography and reactive-ion-beam etching. Characterization revealed a reflectivity of 2% for TE polarization and 23% for TM polarization, a difference in reflectivity of over a factor of ten for the two polarizations. The significant polarization-dependent difference in reflectivity confirms the applicability of these AR surfaces to polarization control in VCSELs.

ACKNOWLEDGMENTS

The authors thank T. R. Carter and S. Samora for expert technical assistance. This work was performed at Sandia National Laboratories which is supported by the U.S. Department of Energy under Contract No. DE-AC04-94AL85000.

[1]K. D. Choquette, R. P. Schneider, Jr., K. L. Lear, and R. E. Leibenguth, IEEE J. Sel. Top. Quantum Electron. **1**, 661 (1995).
[2]M. Born and E. Wolf, *Principles of Optics*, 6th ed. (Pergamon, New York, 1980).
[3]D. C. Flanders, Appl. Phys. Lett. **42**, 492 (1983).
[4]R. C. Enger and S. K. Case, Appl. Opt. **22**, 3220 (1983).
[5]T. K. Gaylord, W. E. Baird, and M. G. Moharam, Appl. Opt. **25**, 4562 (1986).
[6]Y. Ono, Y. Kimura, Y. Ohta, and N. Nishida, Appl. Opt. **26**, 1142 (1987).
[7]L. H. Cescato, E. Gluch, and N. Streibl, Appl. Opt. **29**, 3286 (1990).
[8]D. H. Raguin and G. M. Morris, Appl. Opt. **32**, 1154 (1993).
[9]W. Deng and S. Y. Chou, J. Vac. Sci. Technol. B **13**, 2879 (1995).
[10]R. E. Collin, *Field Theory of Guided Waves*, 2nd ed. (IEEE, New York, 1991).
[11]R. E. Smith, M. E. Warren, J. R. Wendt, and G. A. Vawter, Opt. Lett. **21**, 1201 (1996).
[12]M. E. Warren, R. E. Smith, G. A. Vawter, and J. R. Wendt, Opt. Lett. **20**, 1141 (1995).
[13]J. R. Wendt, G. A. Vawter, R. E. Smith, and M. E. Warren, J. Vac. Sci. Technol. B **13**, 2705 (1995).